JOURNAL OF
Materials
CHEMISTRY

Synthesis of BN-coated CeO_2 fine powder as a new UV blocking material

Toshiyuki Masui,[a] Misa Yamamoto,[a] Takao Sakata,[b] Hirotaro Mori[b] and Gin-ya Adachi*[a]

[a]*Department of Applied Chemistry, Faculty of Engineering, Osaka University, 2-1 Yamadaoka, Suita, Osaka 565-0871, Japan. E-mail: adachi@chem.eng.osaka-u.ac.jp*
[b]*Research Center for Ultra-High Voltage Electron Microscopy, Osaka University, 2-1 Yamadaoka, Suita, Osaka 565-0871, Japan*

Received 13th August 1999, Accepted 25th October 1999

A new UV-blocking material consisting of cerium oxide (ceria) and turbostratic boron nitride (t-BN) has been synthesized. The surface of the ceria powders was coated with a t-BN layer by means of reaction between boric acid and urea on the surface of ceria. The thickness of the t-BN layer estimated by high resolution transmission electron microscopy was *ca.* 10 nm. The BN-coating was very effective in reducing the catalytic activity of the ceria and the resulting matrial showed good light scattering and absorption of UV light. BN-coated ceria particles included in an organic thin film showed higher transparency and blocked UV light more effectively than conventional micronized titanium dioxide or zinc oxide particles, two inorganic materials in common use in cosmetics and in many other applications as UV blocking materials.

1 Introduction

It is well known that ultraviolet (UV) rays cause sunburn and suntanning.[1–3] Sunburn is mainly caused by UV-B radiation (290–320 nm) whereas suntanning is mainly caused by both of UV-B and UV-A radiation (320–400 nm).[1] Although the percentage of UV-B in total UV radiation is only *ca.* 10%,[4] its effect in causing sunburn and to damage DNA is very strong.[1–3] The effect of UV-A to cause sunburn is weak, but UV-A still produces active oxygen which can change the structures of collagen and elastin, oxidize lipids, and also damage DNA.[1–3] Therefore, UV rays in sunlight are important factors which produce skin cancer, accelerate the aging of skin such as through the formation of wrinkles and blotches, and induce other deleterious effects on human skin. Recently, sunscreen products and their degree of efficacy have greatly increased with the spread of consumers' knowledge on the harmful effects of UV rays.

Many organic UV absorbers and inorganic UV blocking materials, such as micronized rutile titanium dioxide (TiO_2) and zinc oxide (ZnO) are used in practical cosmetics.[5] However, organic absorbers may have safety problems when they are used at high concentrations.[6] Titanium dioxide is a very good material for blocking UV rays, but has a high photocatalytic activity.[7] Also, cosmetics incorporating TiO_2 particles produce unnatural pale white colors because of the light reflecting and scattering properties of TiO_2 in the visible region.[8] Clearly this is not good for application to cosmetics. Although ZnO is also well known as a UV blocking material, especially in the UV-A region,[9] it has a high oxidation catalytic activity.[10,11]

Bandgap energies of TiO_2 (rutile) and ZnO, the conventional inorganic UV blocking materials, are 3.0[12,13] and 3.4 eV,[14–16] respectively. Cerium oxide (CeO_2) is also well known as a UV blocking oxide,[17–26] since its bandgap energy is *ca.* 3.1 eV.[20–23] In addition, the refractive index of CeO_2 in the visible region is 2.1–2.2[27,28] which is less than that of rutile TiO_2 (2.5–2.7)[29] and is almost the same as that of ZnO (2.0–2.1).[30] This suggests the transparency of CeO_2 is as the same as that of ZnO which shows a higher transparency than TiO_2 in a form of thin film. As a result, CeO_2 is becoming more prominent as a new UV blocking material for cosmetics. However, CeO_2 fine particles readily aggregate or agglomerate to each other to form hard and rough surfaces,[31,32] leading to lack of smoothness and a hard touch to the skin. In addition, the high catalytic activity of CeO_2[33] may cause oxidation of sebum as well as deterioration of the products. Consequently, there have been only a few studies on the use of cerium dioxide as a UV blocking material for cosmetics.[34,35]

In this study, a new UV blocking material consisting of cerium dioxide (CeO_2) and turbostratic boron nitride (t-BN) has been synthesized by reaction between boric acid and urea on the surface of ceria fine powders. Boron nitride is a chemically and thermally stable white compound which shows good slipperiness, spreading and appropriate covering effects.[36,37] Therefore, it is expected that a surface coating of boron nitride would be effective in whitening ceria powders and to restrain their high catalytic activities.

2 Experimental

Cerium dioxide fine powder (Shin-Nippon Kinzoku Kagaku) with average diameters of 10 and 3.5 µm for primary and secondary particles, respectively, was of $>99.9\%$ purity. Boric acid (Wako Pure Chemical Industries), urea (Wako Pure Chemical Industries) and ethanol (Wako Pure Chemical Industries) of the best quality commercially available were used without further purification. Commercially available TiO_2 (rutile, Wako Pure Chemical), TiO_2 (anatase, Degussa P-25) and ZnO (Sakai Chemical FINEX-25) powders were used for comparison studies.

Cerium dioxide particles (5 g) were ultrasonically dispersed in 200 ml of ethanol containing dissolved boric acid and urea. During the dispersion, 100 ml of deionized water was added to prevent formation and vaporization of boron ethoxide. The amount of boric acid was adjusted so as to correspond to 70 vol% of the obtained powder when all of the boric acid reacted to form boron nitride, while the amount of urea employed for the reaction was twice the stoichiometric value. After ultrasonic dispersion for 1 h, the solvent was distilled off using a rotary evaporator and the obtained powders were vacuum-dried at 353 K for 2 days. The dried powders were heated at 773 K in a nitrogen flow for 3 h and subsequently calcined at the same temperature in air for 3 h. After washing with deionized water and then ethanol, the powders were dried in an oven at 353 K. Pure turbostratic boron nitride was also prepared from 3.8 g of boric acid and 7.4 g of urea in a similar manner to the preparation of the t-BN-coated CeO_2, to compare catalytic activities and surface composition.

The obtained particles were characterized by X-ray diffraction (XRD) using Cu-Kα radiation (MAC Science M18XHF-SHA). The morphology and the surface condition of the particles were observed using a high-resolution electron microscope (HREM) (Hitachi H-9000) operated at 300 kV. The microscope had a point resolution of 0.19 nm. The average size and size distribution of the secondary particles were measured using a particle size analyzer (HORIBA LA-500). Densities were determined by means of a small pycnometer employing water at 298 K. Surface composition and coverage were examined by X-ray photoelectron spectroscopy (XPS) using Mg-Kα radiation (ULVAC 5500MT).

Catalytic activities of the t-BN-coated powders were measured by the conductometric determination method (CDM) which utilized oxidation of castor oil.[34,35,38] This method has been used extensively to determine the oxidative deterioration of fats and oils,[39–41] but it has also been confirmed that this method is effective for estimating the catalytic activity of inorganic pigments for oil containing cosmetics.[38] A sample of 0.3 g of t-BN-coated CeO_2 powder was mixed with 5 g of castor oil and maintained at 403 K[42] with bubbling of air (15 liters h^{-1}) for 3 h with the effluent gas introduced into deionized water placed in an electric conductivity measurement cell. Volatile molecules produced by the oxidation of the castor oil were trapped in the water leading to an increased conductivity. The degree of catalytic activity was estimated by the extent of conductivity change after 3 h oxidation. The photocatalytic activities of the samples were also estimated by light irradiation for 9 h using a solar simulator (Yamashita Denso YSS-80) at room temperature.

Optical properties of the powder and thin film samples were measured with a UV–VIS spectrometer (Shimadzu UV-2000). The optical reflectance of the powder was measured using barium sulfate as a reference. The thin film sample was prepared by application of a mixture of 0.9 g of the BN-coated CeO_2 powder with 2.0 g of castor oil and 10 g of clear lacquer onto a quartz glass plate by dip coating. The thickness of the film was 40 µm. Similar film samples containing TiO_2, ZnO and CeO_2 particles were also prepared adjusting the concentrations of the powders to give the same approximate level of transmittance in the visible region.

3 Results and discussion

3.1 Characteristics of the BN-coated CeO_2 fine powders

Fig. 1 shows the change of the X-ray diffraction patterns during boron nitride formation on the CeO_2 fine powders. The pattern of the CeO_2 fine powder is shown in Fig. 1(a). All of the peaks were broad owing to the small size of the crystallites. Fig. 1(b) shows the pattern of the sample after the evaporation of ethanol and water. The diffraction patterns of boric acid and urea were observed in addition to that of cerium oxide. The peaks of boric acid and urea disappeared after nitrification and calcination and a broad but very weak peak appeared at 2θ *ca.* 25° [Fig. 1(c)] which suggested the formation of turbostratic[43] boron nitride.[44–46] Turbostratic boron nitride (t-BN) has a semi-crystalline structure and is a precursor of hexagonal boron nitride (h-BN).[44–46] The structure of t-BN is analogous to turbostratic carbon black, and can be defined in terms of B_3N_3 hexagonal layers stacked roughly parallel to each other with a random rotation and translation above the layer normal which indicates a two-dimensional ordering of the molecules.[44,45] After t-BN-coating, the cerium oxide powder changed from pale yellow to pale beige.

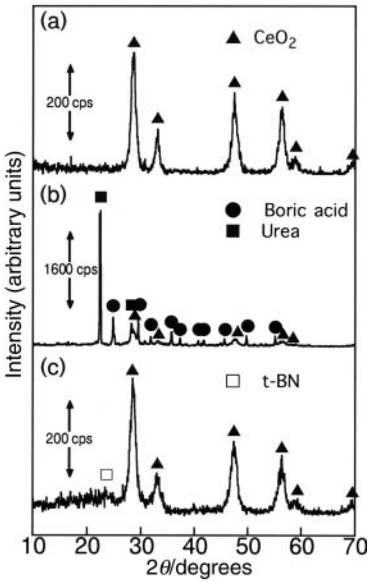

Fig. 1 XRD patterns of t–BN-coated CeO_2 powders: (a) starting CeO_2, (b) precursor before nitriding and subsequent calcination and (c) t-BN-coated CeO_2.

Size distribution histograms of the secondary particles of the starting CeO_2 and t-BN-coated CeO_2 particles are shown in Fig. 2 while the average particle size and density are summarized in Table 1. After the t-BN coating, the amount of smaller particles increased while the average particle size of the samples slightly increased from 3.5 to 4.9 µm. These results

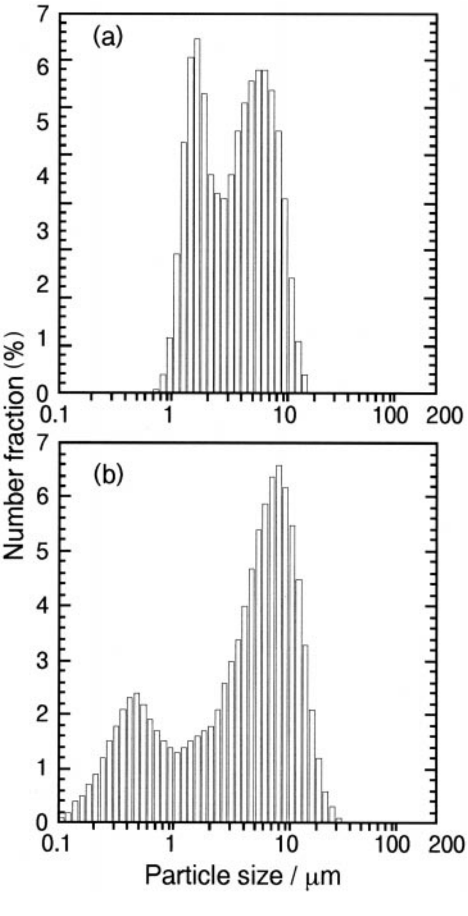

Fig. 2 Secondary particle size distribution histograms of CeO_2 and the BN-coated CeO_2 powder: (a) starting CeO_2 and (b) t-BN-coated CeO_2.

Table 1 Average size and powder density for t-BN-coated CeO_2

Sample	Average size/μm	Powder density/g cm^{-3}
CeO_2	3.5	3.79
t-BN-coated CeO_2	4.9	2.59

suggest that hard aggregation and particle growth of CeO_2 particles were prevented by ultrasonic dispersion and subsequent coating with turbostratic boron nitride. The apparent powder densities of the t-BN-coated CeO_2 powders also decreased upon t-BN-coating.

3.2 HREM and XPS results

Fig. 3 shows a representative high-resolution electron micrograph (HREM) of t-BN-coated CeO_2 powders. The secondary powder consisted of fine CeO_2 primary particles of 10 nm diameter with the surface of the particles covered with a somewhat disordered layer. Crossed lattice fringes corresponding to the {111} reflections (0.31 nm) are seen for the CeO_2 partcles while BN {002} lattice fringes having an interplanar spacing of 0.34 nm were observed in the partially ordered outer surface in the turbostratic boron nitride layer. This interplanar spacing value (0.34 nm) corresponds closely to reported values for hexagonal boron nitride.[47–49] The t-BN film covered the CeO_2 particles with a thickness of *ca.* 10 nm, and was not removed by washing in boiling water. This suggests a tightly adherent coating, although it is difficult to find direct evidence to elucidate the bonding between CeO_2 and t-BN from the HREM image. Direct bonding would appear important, since exfoliation of the t-BN layer would lead to the reappearance of the CeO_2 surface which catalyzes oxidation.

X-Ray photoelectron spectra (XPS) are shown in Fig. 4. Cerium oxide usually shows Ce 3d peaks at *ca.* 880–900 eV with very strong satellite peaks caused by the induced electron transfer from oxygen to cerium.[50] However, the XPS spectrum of the t-BN-coated CeO_2 [Fig. 4(c)] showed, at most, very weak Ce 3d peaks while B 1s and N 1s peaks were prominent. The binding energies of the B 1s and the N 1s peaks were 191.2 and 398.1 eV, respectively, which were slightly larger than those for B 1s (190.3 eV) and N 1s (397.9 eV) reported for hexagonal boron nitride.[50] In comparison, the binding energies of the B 1s and N 1s peaks for turbostratic boron nitride prepared by the reaction of boric acid with urea were 190.6 and 398.0 eV, respectively. Surface compositions of cerium, boron, nitrogen and oxygen of the t-BN-coated CeO_2 and the t-BN powders were determined by the ratio of peak area intensities for Ce 3d : B 1s : N 1s : O 1s and results are summarized in Table 2. The surface coverage of the cerium oxide with turbostratic boron nitride calculated from the Ce 3d intensity was *ca.* 95%. However, the oxygen content is high for both t-BN-coated CeO_2 and t-BN.

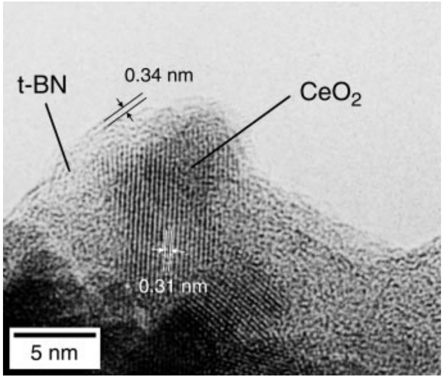

Fig. 3 High–resolution electron micrograph of a t-BN-coated CeO_2 powder.

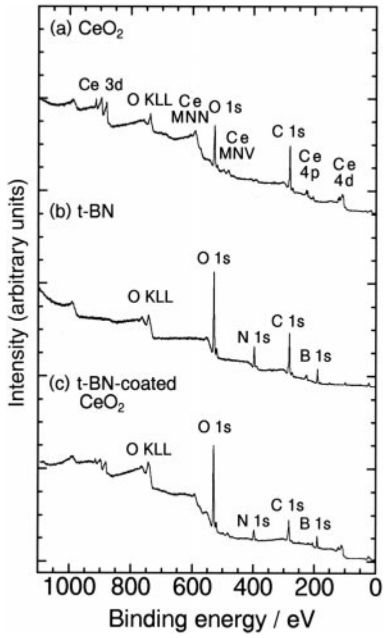

Fig. 4 XPS spectra of CeO_2, t-BN and t-BN-coated CeO_2 powder: (a) starting CeO_2, (b) t-BN and (c) t-BN-coated CeO_2.

Hubácek *et al.*[46,51] reported the presence of oxygen-containing phases interpreted as boron oxynitride and amorphous boric oxide, when turbostratic boron nitride was prepared from boric acid and urea. They elucidated that the products prepared from boric acid and urea at temperatures as low as 493 K had the XRD diffraction patterns of t-BN, and the prepared t-BN showed a high oxygen content of between 28 and 59 atom% which depended on the concentration of urea.[46] In turbostratic boron nitride, boron nitride and amorphous boric oxide phases are interconnected by coordinatively unsaturated dangling bonds at the periphery of the planar boron nitride molecules. Boron oxynitride exists between these two phases but is not an individual compound, rather it represents an interfacial zone present between t-BN and amorphous boric oxide networks. Also, the interfacial zone represents a natural transition from boron nitride to amorphous boric oxide. This specific character of the transition phase was elucidated from IR spectra measurements.[46] The present results obtained from the XPS spectra measurements of the t-BN-coated CeO_2 and the t-BN powders support this explanation, and it is suggested that the small differences of the binding energies and the high oxygen content observed for the t-BN-coated CeO_2 and the t-BN are due to the presence of a substantial amount of residual oxygen from boron oxynitride and amorphous boric oxide phases. Consequently, an explanation for the strong interaction between t-BN and CeO_2 could be attributed to the presence of chemical bonding through bridging oxygen atoms.

3.3 Evaluation of catalytic activities

Catalytic activities of the samples measured by conductometric determination are summarized in Table 3. After oxidation of castor oil for 3 h, the electronic conductivity changes for the t-BN-coated CeO_2 powders were compared with those of TiO_2 (rutile), ZnO, and CeO_2. The starting CeO_2 powders without t-BN-coating showed higher activity than those of the other powders. However, the catalytic activity was decreased after t-BN-coating. The deactivation of the catalysis is in accord with the surface coverage results obtained from the XPS analysis. These results indicate that coating with turbostratic boron nitride is very effective in reducing the high catalytic activity of the CeO_2 powders. The electronic conductivity

Table 2 Surface composition of t-BN-coated CeO_2 and t-BN

	Surface concentration (atom%)			
Sample	Ce 3d	B 1s	N 1s	O 1s
t-BN-coated CeO_2	2.5	32.4	10.9	54.2
t-BN	0	35.4	19.3	45.3

Table 3 Composition of thermal catalytic activities

Sample	Electric conductivity/μS cm^{-1}
t-BN-coated CeO_2	12.5
CeO_2	48.1
t-BN	8.0
TiO_2 (rutile)	13.1
TiO_2 (anatase)	12.0
ZnO	28.5
Castor oil	7.1

change of the t-BN-coated CeO_2 powders upon heating was smaller than that of ZnO and almost equal to those of rutile and anatase TiO_2 powders. Moreover, the t-BN-coated CeO_2, pure CeO_2 and ZnO showed no photocatalytic activity, while TiO_2 had a high photocatalytic activity (Table 4).

3.4 Optical properties

Fig. 5 shows the reflection spectra of pressed powders of t-BN-coated CeO_2 compared with those of pure CeO_2, micronized TiO_2 (rutile) and ZnO powders. In the powder reflection spectra, low reflectance values indicate high absorption in the corresponding wavelength region. Zinc oxide and titanium oxide totally reflected visible light, while the reflectance of pure CeO_2 was reduced below 480 nm. The reflectance of the t-BN-coated CeO_2 in the visible region was lower than those of the above three samples. Taking account of the results for pure CeO_2, this reduction in reflectance can be ascribed to the formation of a turbostratic BN layer on the surface of the cerium oxide. Below 400 nm, the BN-coated CeO_2 powder effectively absorbed UV radiation. In the reflectance spectra there was very little difference among all samples in the UV-B region in the region 290–320 nm, but a clear difference was observed in the UV-A region especially in the region 390–400 nm. As mentioned in the Introduction, titanium dioxide is a very good material for blocking UV radiation, but the effect in blocking UV-A rays above 380 nm was relatively lower than that for the t-BN-coated CeO_2. The wavelength at which the reflectance began to decrease was lower for ZnO than TiO_2 since the bandgap energy of ZnO is higher than that of TiO_2 (rutile),[12–16] but the reflectance fell sharply from 380 to 370 nm. Consequently, the absorption of long wavelength UV light in the region 320–380 nm was greater than that for TiO_2. Cerium oxide and the t-BN-coated CeO_2 showed better absorption over the whole of the UV-A region from 320 to 400 nm than TiO_2 and ZnO, and in particular, the t-BN-coated CeO_2 showed lower reflectance in the long wavelength UV region near 400 nm than the other powders. The high absorption (low reflection) in the UV region for the BN-coated CeO_2 showed that this material was suitable as a UV-blocking material.

Table 4 Comparison of photocatalytic activities

Sample	Electric conductivity/μS cm^{-1}
t-BN-coated CeO_2	4.5
CeO_2	4.9
TiO_2 (rutile)	10.0
TiO_2 (anatase)	13.9
ZnO	5.1
Castor oil	4.1

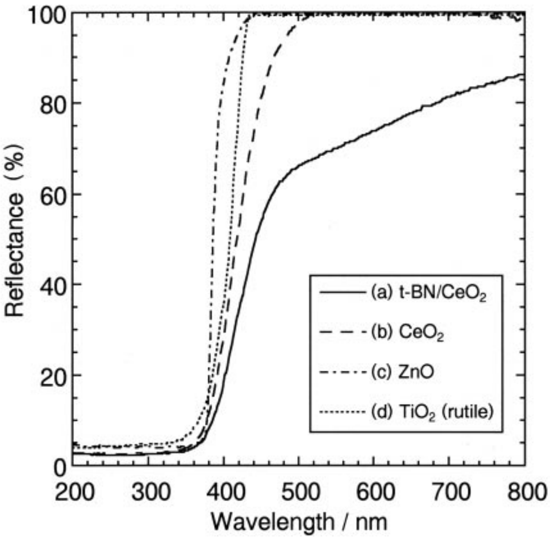

Fig. 5 Reflectance spectra of UV blocking powders: (a) t-BN-coated CeO_2, (b) CeO_2, (c) ZnO and (d) TiO_2 (rutile).

Fig. 6 shows the transmittance of films with thickness of 40 μm. The films were composed of castor oil, clear lacquer and inorganic UV blocking material. The concentrations of the samples containing t-BN–CeO_2, TiO_2 (rutile), ZnO and CeO_2 fine powders were 7, 1, 3 and 5 wt%, respectively. These concentrations were adjusted to give the same approximate level of transmittance in the visible regon for all the films. The low transparency of TiO_2 arises from the high masking property of this material. Generally, TiO_2 shows perfect reflectance in the visible region (Fig. 5) but the material has a high refractive index of *ca.* 2.6.[29] This high refractive index leads to a high degree of masking, and, therefore, it is relatively difficult to obtain high transparency when TiO_2 is applied in the form of thin films. On the other hand, the refractive indices in the visible region of CeO_2 (*ca.* 2.1),[27,28] ZnO (*ca.* 2.0)[30] and BN (*ca.* 1.74)[52] are lower than that of TiO_2, suggesting that thin film samples containing CeO_2, ZnO and t-BN particles should be more transparent in the visible region than films containing TiO_2. The absorbance of the thin film of t-BN–CeO_2 particles started at 400 nm and the transmittance reached zero at 350 nm. This absorption behavior was similar to that of CeO_2. By contrast, absorbance of thin films of TiO_2 (rutile) and ZnO

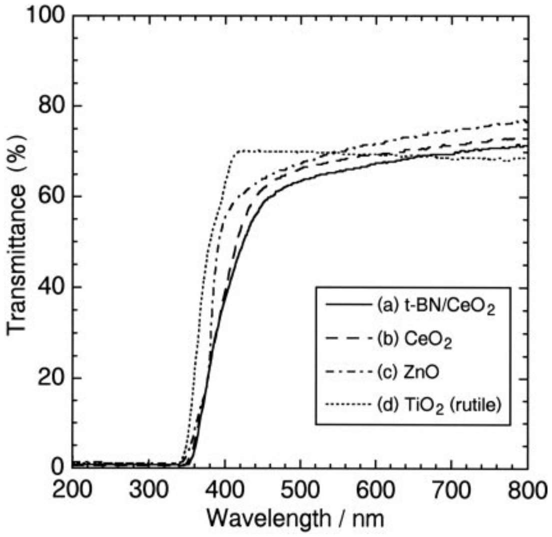

Fig. 6 Transmittance spectra of thin films containing UV blocking particles: (a) 7 wt% t-BN-coated CeO_2, (b) 5 wt% CeO_2, (c) 3 wt% ZnO and (d) 1 wt% TiO_2 (rutile).

started at lower wavelength than for the t-BN-coated sample. As a result, in the long wavelength UV-A region (380–400 nm) the blocking effects of CeO_2 and t-BN–CeO_2 are higher than those of TiO_2 and ZnO.

4 Conclusions

A new material consisting of cerium oxide and turbostratic boron nitride was prepared by chemical reaction of boric acid and urea on the surface of the cerium oxide fine powders. The surface coating with t-BN is very effective in reducing catalysis, is highly transparent, yet shows the good UV blocking property of cerium oxide. The low reactivity is attributed to covering of active catalytic sites by chemical blocking through bridging oxygen atoms while the high transparency is due to the low refractive indices of t-BN and CeO_2 in the visible region. These characteristics suggest that this material is suitable for cosmetics and in many other applications as a UV blocking material.

Acknowledgements

The authors thank Mr Shinryo Yabe (KOSÉ Corporation) for his many useful suggestions for characterization of the catalytic activities. The authors are indebted to Dr Hideki Yoshioka and Dr Hirokazu Izumi (Hyogo Prefectural Institute of Technology) for their assistance with X-ray photoelectron spectroscopy measurements. The authors also thank the Shin-Nippon Kinzoku Kagaku Co., Ltd for supplying starting materials. This work was supported by a Grant-in-Aid for Scientific Researches (B) Nos. 10555304 and 11450335 from the Japan Society for the Promotion of Science.

References

1 J. H. Epstein, in *Sunscreens—Development, Evaluation, and Regulatory Aspects*, ed. N. J. Lowe, N. A. Shaath and M. A. Pathak, Marcel Dekker, New York, 2nd edn., 1997, p. 83.
2 D. P. Meyers, N. J. Lowe and I. R. Scott, in *Sunscreens—Development, Evaluation, and Regulatory Aspects*, ed. N. J. Lowe, N. A. Shaath and M. A. Pathak, Marcel Dekker, New York, 2nd edn., 1997, p. 101.
3 L. H. Kligman and A. M. Kligman, in *Sunscreens—Development, Evaluation, and Regulatory Aspects*, ed. N. J. Lowe, N. A. Shaath and M. A. Pathak, Marcel Dekker, New York, 2nd edn., 1997, p. 117.
4 M. Fukuda, M. Nakagawa and K. Nakajima, *Acta Dermat.*, 1987, **82**, 551.
5 M. W. Anderson, J. P. Hewitt and S. R. Spruce, in *Sunscreens—Development, Evaluation, and Regulatory Aspects*, ed. N. J. Lowe, N. A. Shaath and M. A. Pathak, Marcel Dekker, New York, 2nd edn., 1997, p. 353.
6 R. Hayakawa, M. Kobayashi and K. Matsunaga, *Aller. Prac.*, 1983, **21**, 38.
7 M. R. Hoffman, S. T. Martin, W. Choi and D. W. Bahnemann, *Chem. Rev.*, 1995, **95**, 69.
8 H. Ando, *Fragrance J.*, 1997, **25**, 65.
9 T. Sakurai and K. Saito, *Fragrance J.*, 1999, **27**, 79.
10 O. B. Krylov, *Kinet. Katal.*, 1962, **3**, 502.
11 Y. Noto, K. Fukuda, T. Onishi and K. Tamaru, *Trans. Faraday Soc.*, 1967, **63**, 3081.
12 J. Pascual, J. Camassel and H. Mathieu, *Phys. Rev. B: Condens. Matter*, 1978, **18**, 5606.
13 M. Anpo, T. Shima, S. Kodama and Y. Kubokawa, *J. Phys. Chem.*, 1987, **91**, 4305.
14 D. G. Thomas, *J. Phys. Chem. Solids*, 1960, **15**, 86.
15 Y. S. Park, C. W. Litton, T. C. Collins and D. C. Reynolds, *Phys. Rev.*, 1966, **143**, 512.
16 W. Y. Liang and A. D. Yoffe, *Phys. Rev. Lett.*, 1968, **20**, 59.
17 R. C. Linares, *J. Phys. Chem. Solids*, 1967, **28**, 1285.
18 E. A. Schatz, *J. Am. Ceram. Soc.*, 1968, **51**, 287.
19 R. Haensel, P. Rabe and B. Sonntag, *Solid State Commun.*, 1970, **8**, 1845.
20 C. A. Hogarth and Z. T. Al-Dhhan, *Phys. Status Solidi B*, 1986, **137**, K157.
21 K. B. Sundaram and P. Wahid, *Phys. Status Solidi B*, 1990, **161**, K63.
22 S. Zheng, A. M. Andersson-Fäldt, B. Stjerna and C. G. Granqvist, *Appl. Opt.*, 1993, **32**, 6303.
23 Z. C. Orel and B. Orel, *Phys. Status Solidi B*, 1994, **186**, K33.
24 M. S. Al-Robaee, M. G. Krishna, K. N. Rao and S. Mohan, *J. Vac. Sci. Technol A*, 1991, **9**, 3048.
25 R. M. Bueno, J. M. Martinez-Duart, M. Hernández-Vélez and L. Vázquez, *J. Mater. Sci.*, 1997, **32**, 1861.
26 T. Masui, K. Fujiwara, K. Machida, G. Adachi, T. Sakata and H. Mori, *Chem. Mater.*, 1997, **9**, 2197.
27 G. Hass, J. B. Ramsey and R. Thun, *J. Opt. Soc. Am.*, 1958, **48**, 324.
28 B. T. Kilbourn, *Cerium—A Guide to its Role in Chemical Technology*, Molicorp, Inc. New York, 1992, p. 12.
29 J. R. DeVore, *J. Opt. Soc. Am.*, 1951, **41**, 416.
30 W. L. Bond, *J. Appl. Phys.*, 1965, **36**, 1674.
31 M. Hirano and E. Kato, *J. Am. Ceram. Soc.*, 1996, **79**, 777.
32 M. Hirano and E. Kato, *J. Am. Ceram. Soc.*, 1999, **82**, 786.
33 A. Trovarelli, *Catal. Rev.-Sci. Eng.*, 1996, **38**, 439.
34 S. Yabe and S. Momose, *Sci. Conf. Asian Soc. Cosmet. Sci., 3rd, Taichung, Taiwan*, 1997, p. 103.
35 S. Yabe and S. Momose, *J. Soc. Cosmet. Chem. Jpn.*, 1998, **32**, 372.
36 K. M. Taylor, *Mater. Methods*, 1956, **43**, 88.
37 A. S. Dworkin, D. J. Sasmor and E. R. van Artsdalen, *J. Chem. Phys.*, 1959, **22**, 837.
38 M. Machino and K. Kameyama, *J. Soc. Cosmet. Chem. Jpn.*, 1997, **31**, 329.
39 C. Kato, K. Makabe, H. Katayama, S. Kumita, Y. Takizawa, M. Hara, S. Tanaka, K. Wanaka, K. Watanabe, A. Ohishi, K. Kojima and S. Toukairin, *J. Jpn. Oil Chem. Soc.*, 1993, **42**, 55.
40 D. Barrera-Arellano and W. Esteves, *J. Am. Oil Chem. Soc.*, 1992, **69**, 335.
41 M. H. Gordon and E. Mursi, *J. Am. Oil Chem. Soc.*, 1994, **71**, 649.
42 This temperature is set to accelerate the catalytic reaction. However, this is a minimum temperature to estimate catalytic activity because it is not unusual to use a temperature of >403 K in the manufacturing process of cosmetics.
43 Unordered layer structure, see: J. Biscoe and B. E. Warren, *J. Appl. Phys.*, 1942, **13**, 364.
44 T. E. O'Connor, *J. Am. Chem. Soc.*, 1962, **84**, 1753.
45 J. Thomas, N. E. Weston and T. E. O'Connor, *J. Am. Chem. Soc.*, 1963, **84**, 4619.
46 M. Hubácek, T. Sato and T. Ishii, *J. Solid State Chem.*, 1994, **109**, 384.
47 R. T. Paine, C. K. Narula, R. Shaeffer and A. K. Datye, *Chem. Mater.*, 1989, **1**, 486.
48 A. K. Datye, X. Qiu, T. T. Borek, R. T. Paine and L. F. Allard, *Mater. Res. Soc. Symp. Proc.*, 1990, **180**, 807.
49 T. T. Borek, X. Qiu, L. M. Rayfuse, A. K. Datye, R. T. Paine and L. F. Allard, *J. Am. Ceram. Soc.*, 1991, **74**, 2587.
50 *Handbook of X-ray Photoelectron Spectroscopy*, ed. C. D. Wagner, W. M. Riggs, L. E. Davis, J. F. Moulder and G. E. Muilenberg, Perkin-Elmer, MN, 1978.
51 V. Brozec and M. Hubácek, *J. Solid State Chem.*, 1990, **100**, 120.
52 Y. Shibata and K. Kimura, *Muki Kagaku Zenshyo X-2*, Maruzen, Tokyo, 1965, p. 118.

Paper a906583k